Critical Care

RESEARCH Open Access

AI-driven carotid artery compressibility assessment via point-of-care ultrasound for blood pressure estimation in critically ill and post-resuscitation patients: a prospective observational study

Seung Jin Maeng[1,2†], Subin Park[3†], Ik Joon Jo[1], Guntak Lee[1], Sung Yeon Hwang[1], Myung Jin Chung[4,5,6], Jihyeon Kim[7], Hakje Yoo[4,8*] and Hee Yoon[1,9*]

Abstract

Background Accurate, real-time blood pressure (BP) monitoring is critical in emergency and critical care, but current methods are limited. Invasive arterial catheterization, the gold standard, is often delayed in hypotensive patients, whereas noninvasive cuffs can be unreliable in a state of low perfusion. We hypothesized that carotid artery compressibility measured by point-of-care ultrasound (POCUS) and analyzed via artificial intelligence (AI) could be used to estimate arterial BP noninvasively.

Methods We conducted a prospective observational study enrolling critically ill patients and post-return of spontaneous circulation (ROSC) patients in the emergency department. Standardized POCUS-guided carotid artery compression (POCUS-CAC) was performed. Video clips of POCUS-CAC were analyzed with RealCAC-Net, a deep learning model for quantifying carotid artery compressibility (CAC). The AI-derived maximum CAC value and concurrently measured BP were recorded. Diagnostic and regression analyses were conducted to evaluate the performance of CAC in classifying and predicting BP.

Results A total of 372 ultrasound clips from 56 patients (30 critically ill, 26 post-ROSC) were analyzed. CAC demonstrated strong inverse correlations with systolic ($r = -0.697$), mean ($r = -0.656$), and diastolic ($r = -0.576$) arterial pressures. The model achieved excellent diagnostic performance for identifying hypotension: area under the curve of 0.90 (95% confidence interval (CI), 0.87–0.93) for systolic BP < 60 mmHg and 0.91 (95% CI, 0.88–0.94) for

†Seung Jin Maeng and Subin Park have contributed equally to this work.

*Correspondence:
Hakje Yoo
waihjei11@gmail.com
Hee Yoon
wildhi.yoon@gmail.com

Full list of author information is available at the end of the article

© The Author(s) 2025. **Open Access** This article is licensed under a Creative Commons Attribution-NonCommercial-NoDerivatives 4.0 International License, which permits any non-commercial use, sharing, distribution and reproduction in any medium or format, as long as you give appropriate credit to the original author(s) and the source, provide a link to the Creative Commons licence, and indicate if you modified the licensed material. You do not have permission under this licence to share adapted material derived from this article or parts of it. The images or other third party material in this article are included in the article's Creative Commons licence, unless indicated otherwise in a credit line to the material. If material is not included in the article's Creative Commons licence and your intended use is not permitted by statutory regulation or exceeds the permitted use, you will need to obtain permission directly from the copyright holder. To view a copy of this licence, visit http://creativecommons.org/licenses/by-nc-nd/4.0/.

mean BP < 40 mmHg. Regression models enabled continuous BP estimation with root mean squared errors as low as 8.3 mmHg. The model performed best in hypotensive ranges.

Conclusions This proof-of-concept study demonstrated potential diagnostic utility of carotid artery compressibility for blood pressure estimation in critically ill and post-ROSC patients with hypotensive conditions. Our findings suggest that CAC may provide a noninvasive tool for hemodynamic monitoring, particularly in settings where invasive monitoring is not immediately available. Additional validation studies are warranted.

Keywords Artificial intelligence, Blood pressure estimation, Carotid artery compressibility, Critical care, Point-of-care ultrasound, Cardiac arrest, Hemodynamic monitoring

Graphical abstract

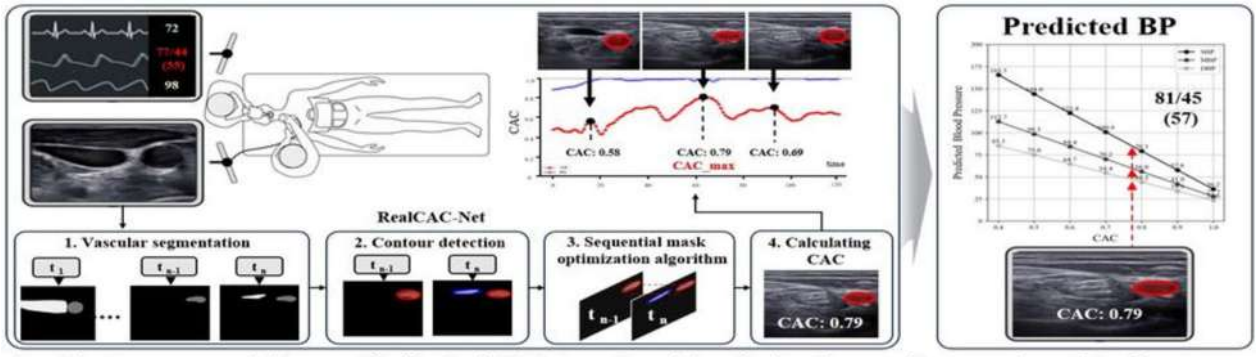

Carotid artery compressibility quantified by RealCAC-Net, an AI model applied to ultrasound images, showed significant correlation with blood pressure, enabling the prediction of pressure ranges.

Background

Accurate and timely assessment of blood pressure is fundamental to the management of critically ill patients [1]. In the emergency department (ED) and intensive care unit, blood pressure serves as a core physiological marker, guiding fluid resuscitation, vasopressor use, and decisions about organ support [2–4]. While invasive arterial catheterization remains the gold standard for continuous blood pressure monitoring, it is technically challenging in hypotensive states, carries procedural risks, and is often delayed during the early phase of resuscitation [5, 6]. Conversely, noninvasive cuff measurements are frequently unreliable in low-perfusion conditions [7, 8]. As such, there remains a clinical gap for a real-time, reliable, noninvasive method to estimate blood pressure, particularly during the crucial moments when treatment decisions must be made rapidly and with incomplete information.

Point-of-care ultrasound (POCUS) has become an indispensable tool in critical care medicine, enabling rapid assessment of volume status, cardiac function, and vascular reactivity [9–12]. Owing to their anatomical accessibility, cervical vessels have been investigated as potential surrogate markers of blood pressure and effective circulatory volume during resuscitation [13–16]. One recent application of POCUS is carotid artery compression (POCUS-CAC), in which the carotid artery is compressed under ultrasound guidance to assess vascular deformation and perfusion dynamics [17]. Our group previously developed RealCAC-Net, an artificial intelligence (AI)-based model that analyzes POCUS-CAC video sequences to assess carotid artery compressibility and determine the presence of return of spontaneous circulation (ROSC) during cardiopulmonary resuscitation (CPR), demonstrating its feasibility for automated, objective pulse assessment [18].

This study originated from a clinical and physiological hypothesis: the degree of carotid artery compressibility—quantified via AI analysis of POCUS-CAC—may reflect not only the presence or absence of circulation, but also the level of underlying arterial blood pressure. Specifically, we posited that hypotensive states would be associated with greater carotid artery deformability under standardized probe pressure, whereas higher blood pressures would produce more resistance to compression. Experimental work with porcine models further supported the physiological plausibility of this hypothesis [19]. This implies that carotid artery compressibility could serve as a continuous surrogate marker of arterial tone, offering a novel approach for estimating blood pressure in settings where invasive access is delayed or unavailable.

To explore this hypothesis, we applied the RealCAC-Net framework to a new prospective dataset comprising critically ill patients with simultaneously measured invasive arterial pressures and ROSC patients with recorded

BP measurements. Our aim was to determine whether AI-analyzed carotid artery compression responses could noninvasively predict arterial blood pressure, and thereby support clinical decision-making during the early and unstable phases of critical illness.

Methods

Study design and ethical approval

This prospective observational study was conducted entirely in the ED of a tertiary academic hospital in Seoul, Korea, to develop a RealCAC-Net based blood pressure prediction model. To ensure broad hemodynamic representation, patients were prospectively enrolled into two cohorts:

- Cohort A (Critically Ill Patients): adult patients requiring invasive arterial blood pressure (ABP) monitoring during acute resuscitation or hemodynamic instability.
- Cohort B (Intra-CPR ROSC Patients): patients who presented to the ED with cardiac arrest, achieved ROSC during ongoing resuscitation, and underwent POCUS-CAC with either invasive or noninvasive blood pressure monitoring during or immediately after CPR.

In both cohorts, bedside POCUS-CAC was performed by trained emergency physicians following a standardized protocol [17, 18].

The study was approved by the Institutional Review Board of Samsung Medical Center (IRB No. 2022-04-018 and 2022-04-016) and was conducted between May 2022 and May 2024. Written informed consent was obtained from participants or their legal surrogates in Cohort A. In Cohort B, the requirement for informed consent was waived due to the emergent nature of cardiac arrest and the use of de-identified data collected during standard resuscitation procedures. All procedures were conducted in accordance with the Declaration of Helsinki.

Patient selection

Cohort A (critically ill patients)

Adult patients (aged ≥ 18 years) who required ABP monitoring in the ED as part of routine clinical care were eligible. Patients were excluded if they had known or suspected carotid artery stenosis, a history of neck surgery or radiation, or structural abnormalities interfering with carotid ultrasound acquisition. Because additional carotid ultrasound to newly diagnose stenosis was not feasible in the emergency setting, exclusion was based on documented or self-reported medical history. Only ultrasound clips and BP measurements obtained within 30 min of arterial catheter placement were included in the analysis.

Cohort B (intra-CPR ROSC patients)

Patients who achieved ROSC following cardiac arrest in the ED were eligible. POCUS-CAC was performed either during CPR at designated pulse check intervals or immediately after ROSC. Both invasive arterial and noninvasive BP measurements were permitted, depending on clinical circumstances. This approach was intended to capture real-time hemodynamic status during the immediate post-cardiac arrest phase, irrespective of monitoring modality. Patients were excluded if carotid ultrasound imaging was technically inadequate or incomplete.

For both cohorts, convenience sampling was used based on the availability of trained research personnel during ED shifts.

Ultrasound and blood pressure acquisition

To ensure standardized acquisition, all participating physicians received a 1-h didactic lecture and hands-on training on the POCUS-CAC technique, including carotid artery localization, appropriate compression pressure, and use of the RealCAC-Net program. Supervised practice was performed on peers, and competency was confirmed before patient enrollment. A total of five emergency physicians participated in this study, including two residents. All ultrasound examinations were performed at the bedside using a linear-array transducer (7–16 MHz; Samsung Ultrasound HM70A, Samsung Healthcare, Seoul, Korea). Following the established POCUS-CAC protocols from previous studies, the transducer was placed transversely across the middle one-third of the patient's neck to simultaneously visualize the common carotid artery and the internal jugular vein (IJV), with the probe marker oriented toward the patient's right (Fig. 1A) [17, 18]. Graded external pressure was applied until the IJV was fully collapsed, and the deformation of the carotid artery was recorded as a dynamic video loop. Each ultrasound clip lasted 3–5 s and was captured at 30 frames per second. Images were saved in Audio Video Interleave format and anonymized for analysis. Systolic, diastolic, and mean blood pressures (SBP, DBP, and MBP) were recorded at the time of POCUS-CAC acquisition.

In Cohort A, the same operator who performed the ultrasound simultaneously observed and documented invasive ABP values displayed on the bedside monitor; monitor files were not exported, and blinding was not feasible. In Cohort B, most patients already had arterial lines in place, and ABP values were directly paired with ultrasound clips at the time of acquisition, including during pulse checks. In cases without arterial lines, NIBP values were obtained as part of routine care almost simultaneously with the ultrasound (within ~1–2 min) and paired with the nearest ultrasound clip.

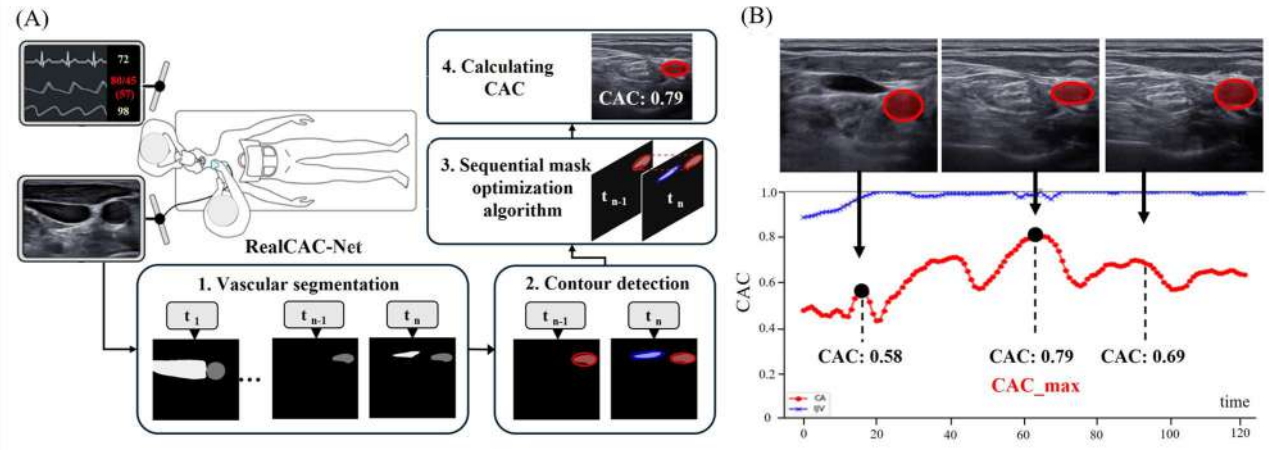

Fig. 1 RealCAC-Net workflow and CAC_max measurement. (**A**) Schematic overview of the RealCAC-Net algorithm pipeline for extracting CAC from POCUS images. The process includes (1) vascular segmentation of ultrasound frames, (2) contour detection of the CA and IJV, (3) sequential mask optimization to ensure temporal consistency across frames, and (4) calculation of CAC based on area changes over the cardiac cycle. (**B**) Representative example of a dynamic CAC waveform. The blue line indicates the compressibility value over time for IJV, an indirect marker of the external pressure applied by the probe. The red line indicates the calculated CAC values over time, and the peak point (CAC_max) is automatically identified. Corresponding ultrasound images show vessel deformation at selected timepoints. CAC, carotid artery compressibility; CAC_max, maximum CAC value during the clip; CA, carotid artery; IJV, internal jugular vein; POCUS, point-of-care ultrasound

Automated AI model-based ultrasound image analysis

All recorded ultrasound video sequences were processed using RealCAC-Net, a previously developed AI model for automated analysis of carotid artery compressibility. The model performs vessel segmentation and quantifies frame-wise deformation of the carotid artery during probe-induced compression. A numerical CAC value was computed for each video, reflecting the extent of carotid artery deformation on a continuous scale (from 0: circular/uncompressed to 1: highly deformed).

The model architecture consists of a TransUNet-based segmentation backbone, which leverages both convolutional neural networks and transformers to identify the carotid artery and IJV from each ultrasound frame [18, 20]. To refine segmentation accuracy and reliably quantify deformation, the CAC measurement algorithm was employed. This algorithm tracks temporal changes in the vessel mask and eliminates frames with low overlap (<50%) between consecutive segmentations to ensure consistency. The vessel contours in each frame were approximated as ellipses, and ellipticity was calculated using the semi-major (a) and semi-minor (b) axes with the formula (e) = $(\mathrm{e}) = \sqrt{1 - \left(\frac{b^2}{a^2}\right)}$. A vessel in a relaxed state retains a near-circular shape, whereas increasing external compression causes elliptical deformation with rising eccentricity. The full pipeline was optimized for real-time performance, processing up to 20 frames per second, enabling prospective CAC quantification at the bedside (Fig. 1A).

Selection of representative CAC metric

From the AI-derived time-series CAC data, we applied several statistical transformations to extract clinically meaningful single-value metrics that reflect vessel deformability under probe-induced compression. As illustrated in Fig. 1B, the CAC curve fluctuated dynamically throughout the cardiac cycle in response to changes in vascular tone and intraluminal pressure. Candidate summary variables included the maximum CAC value during the clip (CAC_max), the CAC value at the frame where the IJV collapsed (CAC_IJV_One), and the ratio of minimum to maximum CAC values (Min_Max_Max). We also evaluated CAC-derived shape metrics such as vessel height and area at maximal compression (Height_Min and Area_Min), the maximal vertical-to-horizontal shape deformation ratio (Height_Width_Max), and the ratio of the initial vessel height to the minimum height during compression (Height_Ratio_First). Pearson correlation coefficients were calculated between each of these variables and the corresponding SBP, MBP, and DBP values. Among all candidates, CAC_max demonstrated the strongest inverse correlation with all three blood pressure indices and was selected as the representative CAC parameter for subsequent analysis.

Statistical analysis

Because this was the first study to evaluate blood pressure prediction using POCUS-CAC, no prior data were available to perform a formal sample size calculation. We initially aimed to collect about 360 clips across six systolic BP ranges (<30, 30–50, 50–70, 70–90, 90–120, and >120 mmHg; 60 clips per group), and enrollment was

closed at the end of a prespecified 2-year study period. The dataset was therefore treated as a convenience sample.

Baseline characteristics were described as medians with their interquartile ranges for continuous variables and as frequencies (percentages) for categorical variables.

Using CAC_max as the representative CAC metric, we evaluated its binary classification performance for identifying blood pressure below guideline-recommended thresholds (e.g., MAP < 65 mmHg, SBP < 90 mmHg) and additional exploratory stepwise increments (10-mmHg for SBP and DBP, 5-mmHg for MAP), thereby including both established clinical targets and transient extremes observed in post-arrest or unstable ED patients [2, 21]. Cases with blood pressure values below each threshold were defined as positive. Receiver operating characteristic (ROC) curve analysis was performed, and area under the curve (AUC) with confidence intervals (CIs), sensitivity, specificity, F1 score, and accuracy were calculated [22]. The Youden index was used to determine the optimal cutoff for each threshold [23].

To further explore the feasibility of continuous blood pressure estimation using CAC metrics, we performed simple linear regression analyses. Separate models were constructed for the overall dataset and for subsets with blood pressure values below each predetermined threshold. Data were split at the patient level into training and validation sets in an 80:20 ratio. Model performance was assessed using the root mean squared error (RMSE) [24]. Predicted blood pressure values were generated across a CAC_max input range of 0.0–1.0 using the regression model to enhance clinical applicability.

All analyses were conducted in Python 3.8 using PyTorch 1.4.0 and standard statistical libraries. A total of 372 ultrasound clips (189 from Cohort A and 183 from Cohort B) were used as the analytic units.

Results

Baseline characteristics

During the study period, 104 patients were screened using convenience sampling. Of these, 56 underwent POCUS-CAC and were included in the final analysis. The remaining 48 patients were excluded due to equipment or personnel limitations, failure to achieve ROSC, insufficient data quality, withdrawal consent or anatomical abnormality (Fig. 2). The final cohort consisted of 30 critically ill patients with invasive arterial monitoring (Cohort A) and 26 patients who achieved ROSC during resuscitation (Cohort B), yielding a total of 372 ultrasound clips (n = 372).

Table 1 summarizes the baseline characteristics. The mean ages in Cohorts A and B were 68 and 67 years, respectively, and 54% of the overall cohort was male. Comorbidities included hypertension (34%), diabetes mellitus (27%), and malignancy (38%), while 20% of the patients had no documented comorbid conditions.

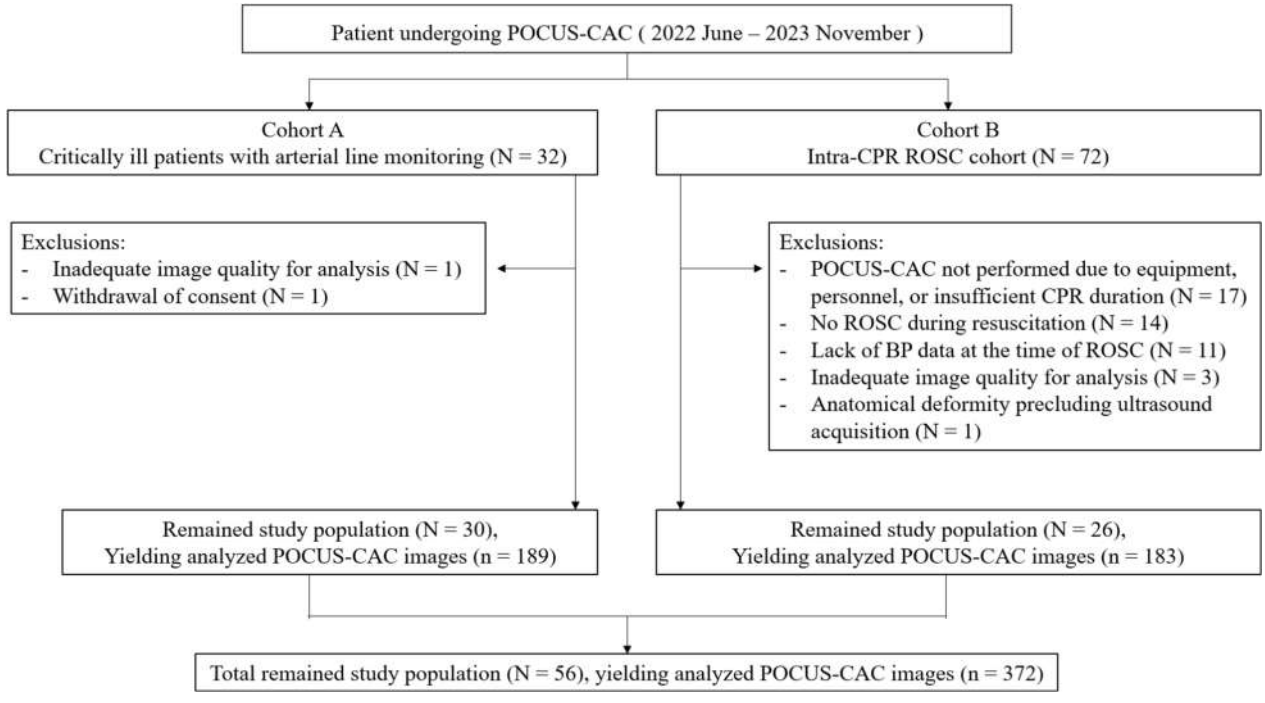

Fig. 2 Patient flowchart for POCUS-CAC analysis. Flowchart summarizing patient enrollment, inclusion criteria, ultrasound acquisition, and data analysis steps. A total of 372 POCUS-CAC video clips were analyzed from 56 critically ill or post-resuscitation patients. POCUS-CAC, point-of-care ultrasound-guided carotid artery compression; ROSC, return of spontaneous circulation; CPR, cardiopulmonary resuscitation

Table 1 Baseline characteristics of study participants (*N* = patients, *n* = clips)

Variable	Cohort A (*N* = 30, *n* = 189)	Cohort B (*N* = 26, *n* = 183)	Total (*N* = 56, *n* = 372)
Demographics	(*N* = 30)	(*N* = 26)	(*N* = 56)
Age (year)	68 (12)	67 (16)	67 (14)
Male sex	14 (47)	16 (62)	30 (54)
Body mass index (kg/m^2)	22 (20–26) (*n* = 23)	22 (20–25) (*n* = 16)	22 (20–25) (*n* = 39)
Comorbidities	(*N* = 30)	(*N* = 26)	(*N* = 56)
Hypertension	12 (40)	7 (27)	19 (34)
Diabetes mellitus	11 (37)	4 (15)	15 (27)
Dyslipidemia	4 (13)	2 (8)	6 (11)
Cardiovascular disease	6 (20)	4 (15)	10 (18)
Chronic pulmonary disease	2 (7)	1 (4)	3 (5)
Chronic liver disease	5 (17)	1 (4)	6 (11)
Chronic kidney disease	3 (10)	2 (8)	5 (9)
Chronic neurological disease	7 (23)	2 (8)	9 (16)
Carotid artery stenosis	NA	0 (0)	NA
Malignancy	11 (37)	10 (38)	21 (38)
None	3 (10)	8 (31)	11 (20)
Arterial line	(*N* = 30)	(*N* = 26)	(*N* = 56)
Location			
Femoral	2 (7)	4 (15)	6 (11)
Radial	26 (87)	17 (65)	43 (77)
Dorsalis pedis	2 (7)	1 (4)	3 (5)
Noninvasive only	NA	3 (12)	NA
Not documented	0 (0)	1 (4)	1 (2)
Cause for placement			
Shock	26 (87)	NA	NA
Hypertensive emergency	1 (3)	NA	NA
Procedural & others	3 (10)	NA	NA
POCUS-CAC imaging	(*n* = 189)	(*n* = 183)	(*n* = 372)
Right-side carotid imaging	84 (44)	104 (57)	188 (51)
Ultrasound operator level			
Resident	8 (4)	0 (0)	8 (2)
EM specialist	181 (96)	183 (100)	364 (98)
Prior POCUS-CAC experience (cases)			
0–5	13 (7)	0 (0)	13 (4)
6–10	11 (6)	0 (0)	11(3)
>10	165 (87)	183 (100)	348 (94)
At time of POCUS-CAC	(*n* = 189)	(*n* = 183)	(*n* = 372)
Systolic blood pressure (mmHg)	100 (83–116)	65 (43–90)	86 (56–109)
Mean blood pressure (mmHg)	67 (58–75)	49 (33–65)	60 (40–74)
Diastolic blood pressure(mmHg)	51 (43–62)	38 (27–52)	46 (32–58)
Heart rate (bpm)	90 (82–115)	NA	NA
Vasopressor use	83 (44)	NA	NA
NEE	0.1 (0.1–0.1) (*n* = 61)	NA	NA

Data are presented as medians (interquartile ranges), or numbers (%), as appropriate. Carotid artery stenosis was one of the exclusion criteria for the critically ill cohort; thus, this value is not applicable (NA) for that group. Selected variables such as heart rate and vasopressor use were available only in the critically ill group. Epinephrine boluses administered during cardiac arrest were not included in the table. NEE was calculated with the equation NEE = Norepinephrine (mcg/kg/min) + Epinephrine (mcg/kg/min) + vasopressin (IU/min) * 2.5. As the critically ill group included only patients with arterial line monitoring, the subcategories 'Noninvasive only' and 'Not documented' for arterial line placement were marked as NA

bpm beats per minute, *CPR* cardiopulmonary resuscitation, *NA* not applicable, *NEE* norepinephrine equivalent dosage, *POCUS-CAC* point-of-care ultrasound-carotid artery compression, *ROSC* return of spontaneous circulation

Carotid artery stenosis was not identified in Cohort B and was an exclusion criterion for Cohort A.

Of the 372 ultrasound clips analyzed, 189 were acquired from Cohort A and 183 were acquired from Cohort B. Right-sided carotid imaging was performed in 51% of clips. Nearly all scans (98%) were performed by board-certified emergency medicine specialists, with 94% conducted by operators who had completed at least 10 POCUS-CAC cases prior to data collection.

At the time of image acquisition, the median systolic, mean, and diastolic blood pressures were 100/67/51 mmHg in Cohort A and 65/49/38 mmHg in Cohort B. Heart rate and vasopressor use were documented only in Cohort A, with a median heart rate of 90 bpm, and vasopressors were administered in 44% of cases. In Cohort B, epinephrine boluses were routinely administered during resuscitation per current Advanced Cardiovascular Life Support guidelines, but the exact timing relative to ultrasound acquisition could not be verified [21]. Arterial lines were most commonly placed in the radial artery (43 patients, 77%), followed by the femoral (6 patients, 11%) and dorsalis pedis (3 patients, 5%) arteries. In Cohort B, noninvasive BP measurements were used in 3 patients (12%), and insertion sites were undocumented in 1 patient (4%).

Correlation between CAC and blood pressure

Table 2 summarizes the Pearson correlation coefficients between various CAC-derived parameters and invasively measured SBP and MBP. Among all tested metrics, CAC_max, exhibited the strongest inverse correlation with SBP (r = −0.697), MBP (r = −0.656), and DBP (r = −0.576). Other parameters, such as CAC_IJV_One, Min_Max_Max, and Height_Width_Max, also showed moderate negative correlations (mean $r \approx$ −0.522 and −0.492

Table 2 Correlation coefficients between CAC parameters and SBP, DBP, and MBP

	SBP	DBP	MBP
Maximum CAC during the clip	−0.697	−0.576	−0.656
CAC at the onset of IJV collapse	−0.548	−0.449	−0.515
Minimum-to-maximum ratio of CAC	−0.511	−0.429	−0.482
Minimum CA height	0.054	0.079	0.077
Minimum CA area	0.257	0.234	0.259
Maximum height-to-width ratio of CA	−0.509	−0.428	−0.480
Ratio of initial to minimum CA height	0.049	0.093	0.076

The values are Pearson correlation coefficients between CAC parameters and blood pressure indices

CAC carotid artery compressibility, *SBP* systolic blood pressure, *DBP* diastolic blood pressure, *MBP* mean blood pressure

for SBP and MBP, respectively). In contrast, Height_Min and Height_Ratio_First showed negligible correlations (mean $r \approx 0.05$ and 0.07), while Area_Min demonstrated a weak positive correlation (mean $r \approx 0.25$). Based on these results, CAC_max was selected as the representative metric for further analyses, as it showed the strongest and most consistent inverse association with arterial blood pressure. To simplify terminology, CAC_max is hereafter referred to as CAC throughout the remainder of the manuscript.

Diagnostic performance of CAC for blood pressure threshold classification

We evaluated the ability of CAC, to identify optimal binary blood pressure thresholds. Supplementary Table 1 summarizes the diagnostic performance of CAC for classifying SBP, DBP, and MBP below each clinical cutoff, and Fig. 3 displays ROC curves illustrating the binary classification performance of CAC across multiple thresholds.

For SBP, the highest AUC values (0.90; 95% CI, 0.87–0.93) were observed at thresholds of 60 mmHg and 70 mmHg, with a progressive decline in AUC at thresholds ≥ 80 mmHg. For DBP, the peak AUC was 0.88 (95% CI, 0.85–0.92) at the 30-mmHg threshold, followed by slightly lower values at 20 mmHg (AUC 0.86; 95% CI, 0.81–0.90) and 40 mmHg (AUC 0.85; 95% CI, 0.80–0.89). At higher thresholds (50 mmHg and 60 mmHg), performance decreased with AUCs of 0.74 (95% CI, 0.69–0.79) and 0.77 (95% CI, 0.70–0.82), respectively. For MBP, the highest AUC values were achieved at 40 mmHg (0.91; 95% CI, 0.88–0.94) and 45 mmHg (0.91; 95% CI, 0.87–0.94), with values remaining stable (AUC 0.90) at lower thresholds (30–35 mmHg) before gradually declining at thresholds approaching 65 mmHg. Overall, a consistent pattern was observed across all blood pressure indices, with lower thresholds associated with increased AUC and sensitivity, highlighting the superior discriminative power of CAC in identifying severe hypotension.

Linear regression models for predicting SBP, DBP, and MBP

Figure 4 and Supplementary Table 2 present the results of linear regression analysis using CAC to predict SBP, DBP, and MBP. Regression models were trained on data subsets with blood pressure values below each predeterminedthreshold. It demonstrated the lowest RMSE values, indicating improved predictive accuracy in hypotensive ranges, whereas performance declined at higher thresholds. The models were trained using the entire dataset. Across all three blood pressure indices, an inverse relationship was observed—higher CAC values were associated with lower blood pressure readings.

The derived regression equations were as follows:

- SBP = −221.08 × CAC + 254.78
- DBP = −106.75 × CAC + 129.02
- MBP = −146.27 × CAC + 172.25

The scatter plots demonstrated moderate dispersion across the range of values. Notably, greater variability was observed in the higher blood pressure ranges, whereas

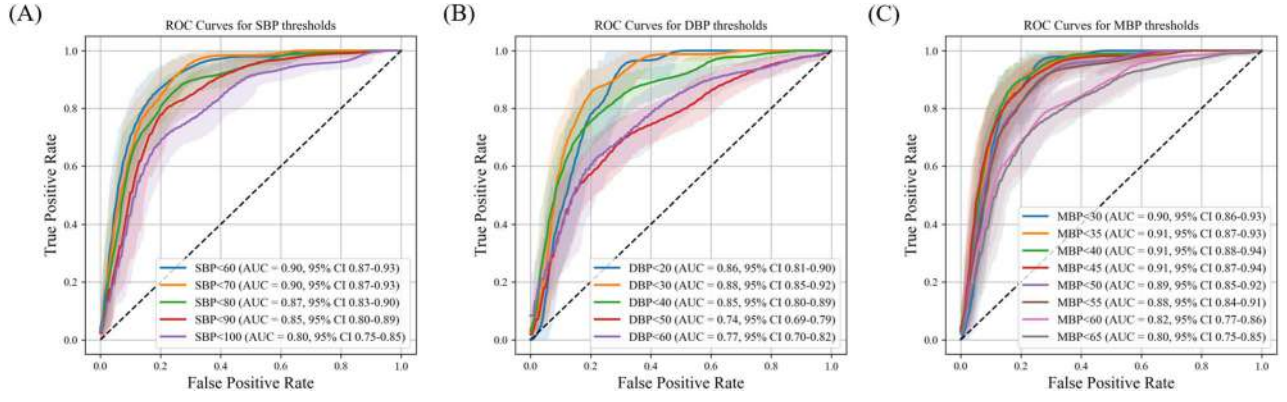

Fig. 3 ROC curves are shown for CAC in the binary classification of hypotension at various thresholds for (**A**) SBP, (**B**) MBP, and (**C**) DBP. The highest diagnostic performance was observed at lower blood pressure thresholds. AUC, area under the curve; CAC, carotid artery compressibility; CI, confidence interval; DBP, diastolic blood pressure; MBP, mean blood pressure; ROC, receiver operating characteristic; SBP, systolic blood pressure.

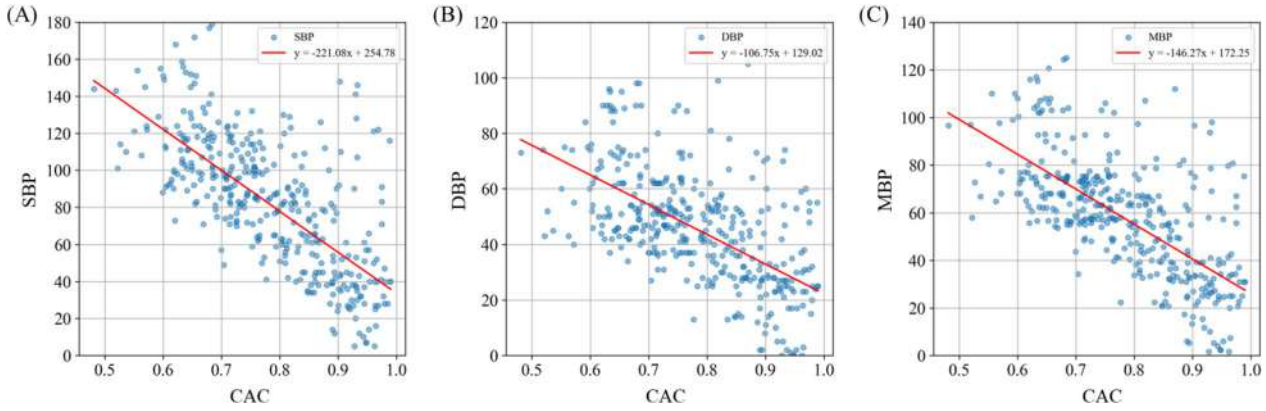

Fig. 4 Scatter plots and linear regression models for CAC and blood pressure. Scatter plots show the inverse relationships between CAC and (**A**) SBP, (**B**) DBP, and (**C**) MBP. Regression lines and equations are included. Greater dispersion was observed in higher blood pressure ranges, while tighter clustering was noted in hypotensive states. CAC, carotid artery compressibility; SBP, systolic blood pressure; DBP, diastolic blood pressure; MBP, mean blood pressure

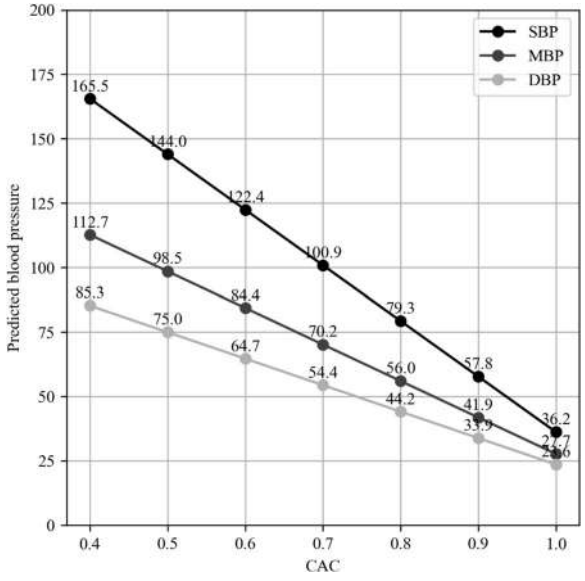

Fig. 5 Predicted blood pressure values using CAC. Linear regression-based prediction curves for SBP, MBP, and DBP across CAC values (0.4–1.0). All pressure indices decline proportionally as CAC increases, with approximately 9.0%, 8.6%, and 7.7% reductions per 0.1-unit increase in CAC for SBP, MBP, and DBP, respectively. CAC, Carotid artery compressibility; SBP, systolic blood pressure; DBP, diastolic blood pressure; MBP, mean blood pressure

lower ranges exhibited tighter clustering, suggesting improved model consistency in hypotensive states.

Blood pressure prediction based on CAC

Figure 5 presents the predicted values of SBP, DBP, and MBP across a range of CAC values (0.4–1.0), derived from the linear regression equations. As CAC increased, all three blood pressure values linearly decreased. For every 0.1 increment in CAC, SBP, DBP, and MBP decreased by approximately 9.0%, 7.7%, and 8.6%, respectively. At the minimum CAC value of 0.4, the predicted SBP, DBP, and MBP were 1663 mmHg, 86 mmHg, and 114 mmHg, respectively. At the maximum CAC of 1.0, the predicted values declined to 34 mmHg, 22mmHg, and 26 mmHg. These findings illustrate the inverse relationship between CAC and blood pressure and support its potential use in estimating circulatory status noninvasively.

Discussion

This prospective study evaluated the feasibility of using AI-analyzed carotid artery compressibility, derived from POCUS-CAC, to estimate blood pressure in critically ill and post-resuscitation patients. Our findings support the physiological hypothesis that vascular deformability, as quantified by CAC, inversely correlates with blood pressure primarily in states of low BP and profound hypoperfusion, and may serve as a surrogate marker when invasive monitoring is unavailable or delayed in states of severe hypotension.

The core physiologic principle underlying our study is that lower intravascular pressures reduce the transmural tension of the carotid artery wall, rendering the vessel more deformable under standardized external compression [25–27]. This was quantitatively captured by CAC, which exhibited the strongest inverse correlation with all three BP indices: systolic (r = −0.697), mean (r = −0.656), and diastolic (r = −0.576) pressures. In contrast, other shape-based parameters derived from AI-assisted vessel tracking, such as minimum height, area, and vertical-to-horizontal ratios, demonstrated limited correlations. This highlights that overall deformability, rather than absolute geometry or dimension, better reflects underlying hemodynamic status. Because CAC quantifies resistance to a transient external load, it behaves as a "systolic-weighted" index—explaining weaker linkage to DBP.

Building on this physiologic foundation, we assessed the diagnostic utility of CAC for identifying hypotensive conditions. The diagnostic performance of CAC for

detecting hypotension was notable, with AUC values exceeding 0.9 for thresholds such as SBP < 60 mmHg and MBP < 40 mmHg. Optimal cutoff values (e.g., CAC >0.827 for SBP < 60 mmHg) may inform early therapeutic decisions in emergent situations when invasive arterial access is not yet established. The ability to predict such thresholds with high sensitivity is particularly valuable in emergent conditions where treatment must be initiated before invasive lines can be placed. Such a capability is particularly beneficial in emergent or resource-limited settings, where early recognition of shock is critical for guiding timely interventions.

Regression modeling further confirmed that CAC can be used to quantitatively estimate SBP, DBP, and MBP, particularly in hypotensive ranges. The lowest RMSEs (e.g., RMSE = 8.302 mmHg for MBP < 30 mmHg) were observed in these critically low blood pressure states. However, the scatter plots (Fig. 4) revealed a threshold phenomenon: above a certain SBP level (~140–180 mmHg), CAC values plateaued in the range of 0.5–0.7. The lowest observed CAC in the dataset was approximately 0.48, even in the highest SBP cases. This implies that the carotid artery resists further compression beyond a certain pressure, limiting CAC's sensitivity to changes in the upper BP range. Consequently, regression models trained on lower-pressure data outperformed those including normotensive or hypertensive cases, as shown in supplementary Table 2.

Figure 5 translates the regression equations into a visual nomogram, allowing clinicians to read-off predicted SBP, MBP, and DBP directly from observed CAC values. The tool is intentionally simple—each 0.1 rise in CAC corresponds to an approximately linear drop in all three pressure indices—to facilitate rapid bedside application. Two limitations, however, must frame its use. First, because the dataset contained no CAC values <0.48, predictions in that range are extrapolations rather than empirical estimates. Second, once SBP surpasses ~140 mmHg, the plateau in CAC markedly diminishes sensitivity to additional pressure changes. Accordingly, the nomogram is most accurate for identifying and trending hypotension or borderline perfusion, while estimates in normotensive or hypertensive states should be interpreted with caution. Nevertheless, CAC-based visual tools enable the indirect estimation of blood pressure using only ultrasound images, providing a practical and intuitive clinical aid for rapid assessment of blood pressure.

These results extend the application of RealCAC-Net beyond binary pulse checks, demonstrating that AI-enhanced POCUS-CAC can deliver continuous, central hemodynamic information without additional hardware [18]. Unlike oscillometric cuffs—or cuff-less wearables that depend on peripheral signals prone to failure during shock—CAC interrogates carotid wall compliance directly and therefore remains interpretable even when peripheral perfusion is poor [8, 28, 29]. This distinction is crucial during resuscitation, when hemodynamics can shift minute-to-minute and rapid therapeutic decisions are required.

Although invasive arterial lines remain the reference standard, our series included a small subset of intra-CPR ROSC patients monitored only with non-invasive cuffs. In that context, CAC still yielded coherent estimates, illustrating its potential when arterial access is delayed or impractical. Because CAC is derived from images that clinicians already acquire for other bedside questions, adding the algorithm incurs no workflow penalty, avoids cuff inflation–deflation cycles, and is less vulnerable to motion artifact.

This study has several limitations. First and foremost, this study is done by the small patient population in single tertiary academic center, using convenience sampling without a priori sample size calculation, with the heterogeneity in blood pressure measurement methods (arterial vs. noninvasive, variable timing relative to ROSC). These factors may threaten generalizability and validity, increase risk of bias, and have contributed to overfitting of the current model. Accordingly, the present findings should be considered proof-of-concept, requiring more rigorous derivation and external validation before clinical application. Second, inter-operator variability and inter-patient correlation may have introduced measurement bias. Although all operators underwent standardized training for probe compression, the degree of applied pressure may still vary. In addition, multiple clips were obtained per patient, which may introduce intra-patient correlation and have biased statistical estimates that assume independence. Third, timing variability may have affected accuracy. The current analysis was based on a static probe-induced compression protocol, which does not capture dynamic changes in vessel compliance. In the post-ROSC cohort, BP values were paired with ultrasound clips obtained almost simultaneously, but given the rapid fluctuations after epinephrine administration may have led to minor temporal variability. Forth, we only perform a quality assurance review of algorithm outputs with small number of test samples; an independent quality assurance process would further strengthen its application to new patient populations. Finally, clinical outcomes such as vasopressor titration, organ perfusion, or overall hemodynamic management were not directly assessed in relation to CAC-based estimations. These represent important endpoints for future validation.

Despite these limitations, our results demonstrate that AI-based analysis of carotid artery compressibility provides a feasible and potentially valuable adjunct for noninvasive blood pressure estimation in hypotensive conditions. More broadly, embedding CAC analytics into

handheld or cart-based ultrasound platforms could provide continuous trend displays and automated hypotension alerts, guiding vasopressor initiation, titration, and response assessment particularly in critically ill or unstable patients where rapid assessment is essential.

Conclusions

In conclusion, this proof-of-concept study demonstrated potential diagnostic utility in hypotensive states of carotid artery compressibility for blood pressure estimation in critically ill and post-ROSC patients. Our findings suggest that CAC may provide a noninvasive tool for hemodynamic monitoring, particularly in settings where invasive monitoring is not immediately available. Furthermore, future studies should validate AI-analyzed carotid artery compressibility for predicting blood pressure in hypotensive conditions in larger cohort and evaluate its feasibility in clinical settings.

Abbreviations

ABP	Invasive arterial blood pressure
AI	Artificial intelligence
Area_Min	Area of carotid artery at maximal compression
AUC	Area under the curve
BP	Blood pressure
bpm	Beats per minutes
CA	Carotid artery
CAC	Carotid artery compressibility
CAC_IJV_One	The CAC value at the frame where the IJV collapsed
CAC_max	Maximum CAC value during the clip
CPR	Cardiopulmonary resuscitation
DBP	Diastolic blood pressure
ED	Emergency department
Height_Min	Height of carotid artery at maximal compression
Height_Ratio_First	The ratio of the initial vessel height to the minimum height during compression
Height_Width_Max	The maximal vertical-to-horizontal shape deformation ratio of carotid artery during carotid artery compression
IJV	Internal jugular vein
MBP	Mean blood pressure
Min_Max_Max	The ratio of minimum to maximum CAC values
NA	Not applicable
NEE	Norepinephrine equivalent dosage
NIBP	Noninvasive blood pressure
POCUS	Point-of-care ultrasound
POCUS-CAC	POCUS-guided carotid artery compression
RMSE	Root mean squared error
ROC	Receiver operating characteristic
ROSC	Return of spontaneous circulation
SBP	Systolic blood pressure

Supplementary Information

The online version contains supplementary material available at https://doi.org/10.1186/s13054-025-05772-2.

Additional file 1.

Acknowledgements

This research was supported by the National Research Foundation of Korea (NRF) grant funded by the Ministry of Science and ICT (MSIT) (No. NRF-2022R1C1C1011864).

Author contributions

Conceptualization, Yoon H.; methodology, Yoon H.; formal analysis, Park SB., Yoo H., Yoon H; data curation, Yoon H., Kim JH.; fund acquisition, Yoon H.; writing–original draft preparation, Park SB, Maeng SJ., Yoo H., and Yoon H.; writing–review and editing, Jo IJ., Yoon H., Maeng SJ., Lee G., Hwang SY. Chung MJ.; supervision: Yoon H and Yoo H.

Funding

This work was supported by a National Research Foundation of Korea (NRF) grant funded by the Ministry of Science and ICT (MSIT) (NRF-2022R1C1C1011864). Funder has no specific role in the conceptualization, design, data collection, analysis, decision to publish, or preparation of the manuscript.

Data availability

De-identified datasets used and/or analyzed during the current study are available from the corresponding author upon reasonable request.

Declarations

Ethics approval and consent to participate

The study was approved by the Institutional Review Board of Samsung Medical Center (IRB No. 2022-04-018 and 2022-04-016) and was conducted between May 2022 and May 2024. Written informed consent was obtained from participants or their legal surrogates in Cohort A. In Cohort B, the requirement for informed consent was waived due to the emergent nature of cardiac arrest and the use of de-identified data collected during standard resuscitation procedures. All procedures were performed in accordance with the principles of the Declaration of Helsinki.

Consent for publication

Not applicable.

Competing interests

The authors declare no competing interests.

Author details

[1]Department of Emergency Medicine, Samsung Medical Center, Sungkyunkwan University School of Medicine, 115 Irwon-ro, Gangnam-gu, Seoul 06351, Republic of Korea
[2]Department of Emergency Medicine, College of Medicine, Graduate School, Kyung Hee University, Seoul 02447, Republic of Korea
[3]Department of Health Sciences and Technology, SAIHST, Sungkyunkwan University, Seoul 06355, Republic of Korea
[4]Medical AI Research Center, Research Institute for Future Medicine, Samsung Medical Center, 81 Irwon-ro, Gangnam-gu, Seoul 06351, Republic of Korea
[5]Department of Radiology, Samsung Medical Center, Sungkyunkwan University School of Medicine, Seoul 06351, Republic of Korea
[6]Department of Data Convergence and Future Medicine, Sungkyunkwan University School of Medicine, Seoul 06351, Republic of Korea
[7]Research Institute for Future Medicine, Samsung Medical Center, Seoul 06351, Republic of Korea
[8]Department of Bio-Mechatronic Engineering, College of Biotechnology and Bioengineering, Sungkyunkwan University, 2066 Seobu-ro, Jangan-gu, Suwon-si, Gyeonggi-do 16419, Republic of Korea
[9]Department of Emergency Medicine, Denver Health, Denver, CO 80204, USA

Received: 31 July 2025 / Accepted: 15 November 2025
Published online: 28 November 2025

References

1. Xiao L, Shen P, Han X, Yu Y. Association between delayed invasive blood pressure monitoring and all-cause mortality in intensive care unit patients with sepsis: a retrospective cohort study. Front Med (Lausanne). 2024;11:1446890. https://doi.org/10.3389/fmed.2024.1446890.
2. Singer M, Deutschman CS, Seymour CW, Shankar-Hari M, Annane D, Bauer M, et al. The third international consensus definitions for sepsis and septic shock

(Sepsis-3). JAMA. 2016;315(8):801–10. https://doi.org/10.1001/jama.2016.0287.
3. Sinha SS, Morrow DA, Kapur NK, Kataria R, Roswell RO. concise clinical guidance: an ACC expert consensus statement on the evaluation and management of cardiogenic shock: a report of the American College of Cardiology Solution Set Oversight Committee. J Am Coll Cardiol. 2025. https://doi.org/10.1016/j.jacc.2025.02.018.
4. Yu Y, Gong Y, Hu B, Ouyang B, Pan A, Liu J, et al. Expert consensus on blood pressure management in critically ill patients. J Intensive Med. 2023. https://doi.org/10.1016/j.jointm.2023.06.001.
5. Schults JA, Young ER, Marsh N, Larsen E, Corley A, Ware RS, et al. Risk factors for arterial catheter failure and complications during critical care hospitalisation: a secondary analysis of a multisite, randomised trial. J Intensive Care. 2024;12(1):12. https://doi.org/10.1186/s40560-024-00719-1.
6. Wang A, Hendin A, Millington SJ, Koenig S, Eisen LA, Shiloh AL. Better with ultrasound: arterial line placement. Chest. 2020. https://doi.org/10.1016/j.chest.2019.08.2209.
7. Keville MP, Gelmann D, Hollis G, Beher R, Raffman A, Tanveer S, et al. Arterial or cuff pressure: clinical predictors among patients in shock in a critical care resuscitation unit. Am J Emerg Med. 2021;46:109–15. https://doi.org/10.1016/j.ajem.2021.03.012.
8. Perera Y, Raitt J, Poole K, Metcalfe D, Lewinsohn A. Non-invasive versus arterial pressure monitoring in the pre-hospital critical care environment: a paired comparison of concurrently recorded measurements. Scand J Trauma Resusc Emerg Med. 2024;32(1):77. https://doi.org/10.1186/s13049-024-01240-y.
9. Ahn JH, Jeon J, Toh H-C, Noble VE, Kim JS, Kim YS, et al. Search 8Es: a novel point of care ultrasound protocol for patients with chest pain, dyspnea or symptomatic hypotension in the emergency department. PLoS One. 2017. https://doi.org/10.1371/journal.pone.0174581.
10. Kok B, Wolthuis D, Bosch F, van der Hoeven H, Blans M. POCUS in dyspnea, nontraumatic hypotension, and shock; a systematic review of existing evidence. Eur J Intern Med. 2022;106:9–38. https://doi.org/10.1016/j.ejim.2022.07.017.
11. Diaz-Gomez JL, Mayo PH, Koenig SJ. Point-of-care ultrasonography. N Engl J Med. 2021;385(17):1593–602. https://doi.org/10.1056/NEJMra1916062.
12. Choi W, Cho YS, Ha YR, Oh JH, Lee H, Kang BS, et al. Role of point-of-care ultrasound in critical care and emergency medicine: update and future perspective. Clin Exp Emerg Med. 2023;10(4):363. https://doi.org/10.15441/ceem.23.101.
13. Chawang HJ, Kaeley N, Bhardwaj BB, Chauhan U, Baid H, Asokan R, et al. Ultrasound-guided estimation of internal jugular vein collapsibility index in patients with shock in emergency department. Turk J Emerg Med. 2022;22(4):206–12. https://doi.org/10.4103/2452-2473.357352.
14. Jaffe A, Goryachev I, Sodini C, Anthony BW. Central venous pressure estimation with force-coupled ultrasound of the internal jugular vein. Sci Rep. 2023;13(1):1500. https://doi.org/10.1038/s41598-022-22867-w.
15. Zakrzewski AM, Huang AY, Zubajlo R, Anthony BW. Real-time blood pressure estimation from force-measured ultrasound. IEEE Trans Biomed Eng. 2018;65(11):2405–16. https://doi.org/10.1109/TBME.2018.2873297.
16. Jaffe AT, Zubajlo RE, Daniel L, Anthony BW. Automated force-coupled ultrasound method for calibration-free carotid artery blood pressure estimation. Ultrasound Med Biol. 2022;48(9):1806–21. https://doi.org/10.1016/j.ultrasmedbio.2022.05.006.
17. Kang SY, Jo IJ, Lee G, Park JE, Kim T, Lee SU, et al. Point-of-care ultrasound compression of the carotid artery for pulse determination in cardiopulmonary resuscitation. Resuscitation. 2022;179:206–13. https://doi.org/10.1016/j.resuscitation.2022.06.025.
18. Park S, Yoon H, Kang SY, Jo IJ, Heo S, Chang H, et al. Artificial intelligence-based evaluation of carotid artery compressibility via point-of-care ultrasound in determining the return of spontaneous circulation during cardiopulmonary resuscitation. Resuscitation. 2024;202:110302. https://doi.org/10.1016/j.resuscitation.2024.110302.
19. Yossef OE, Farajian M, Gilad I, Willenz U, Gutman N, Yosibash Z. Further experimental evidence of the compressibility of arteries. J Mech Behav Biomed Mater. 2017;65:177–89. https://doi.org/10.1016/j.jmbbm.2016.08.013.
20. Chen J, Lu Y, Yu Q, Luo X, Adeli E, Wang Y, et al. Transunet: Transformers make strong encoders for medical image segmentation. arXiv:210204306. 2021. https://doi.org/10.48550/arXiv.2102.04306.
21. Perman SM, Soar J, Donnino MW, Berg KM, Chan PS, Guerguerian AM, et al. 2023 American Heart Association focused update on adult advanced cardiovascular life support: an update to the American Heart Association guidelines for cardiopulmonary resuscitation and emergency cardiovascular care. Circulation. 2023;148(24):e544–57. https://doi.org/10.1161/CIR.0000000000001194.
22. Fawcett T. An introduction to ROC analysis. Pattern Recognit Lett. 2006;27(8):861–74. https://doi.org/10.1016/j.patrec.2005.10.010.
23. Youden WJ. Index for rating diagnostic tests. Cancer. 1950;1:32–5.
24. Chai T, Draxler RR. Root mean square error (RMSE) or mean absolute error (MAE)? Arguments against avoiding RMSE in the literature. Geosci Model Dev. 2014;7(3):1247–50. https://doi.org/10.5194/gmd-7-1247-2014.
25. Joseph J, Pm N, Shah MI, Sivaprakasam M. Arterial compliance probe for cuffless evaluation of carotid pulse pressure. PLoS One. 2018;13(8):e0202480. https://doi.org/10.1371/journal.pone.0202480.
26. Xu C, Xiong H, Gao Z, Liu X, Zhang H, Zhang Y, et al. Beat-to-beat blood pressure and two-dimensional (axial and radial) motion of the carotid artery wall: physiological evaluation of arterial stiffness. Sci Rep. 2017;7(1):42254. https://doi.org/10.1038/srep42254.
27. Zakrzewski AM, Anthony BW. Noninvasive blood pressure estimation using ultrasound and simple finite element models. IEEE Trans Biomed Eng. 2017;9:2011–22. https://doi.org/10.1109/TBME.2017.2714666.
28. Dias FM, Cardenas DA, Toledo MA, Oliveira FA, Ribeiro E, Krieger JE, et al. Exploring the limitations of blood pressure estimation using the photoplethysmography signal. Physiol Meas. 2025. https://doi.org/10.1088/1361-6579/adcb86.
29. Sel K, Osman D, Huerta N, Edgar A, Pettigrew RI, Jafari R. Continuous cuffless blood pressure monitoring with a wearable ring bioimpedance device. NPJ Digit Med. 2023;6(1):59. https://doi.org/10.1038/s41746-023-00796-w.

Publisher's Note

Springer Nature remains neutral with regard to jurisdictional claims in published maps and institutional affiliations.